Configuration Control Experiments in Heliotron J

Tohru MIZUUCHI, Shinji KOBAYASHI, Hiroyuki OKADA, Kazunobu NAGASAKI,
Satoshi YAMAMOTO, Gen MOTOJIMA[b], Shinya WATANABE[c], Kiyofumi MUKAI[c],
Katsuyuki HOSAKA[c], Yusuke KOWADA[c], Shiori MIHARA[c], Akinobu MATSUYAMA[c],
Yuji NAKAMURA[c], Kiyoshi HANATANI, Yasuhiro SUZUKI[b], Masayuki YOKOYAMA[b],
Angela C. FERNÁNDEZ[d], Álvaro A. CAPPA[d], Shigeru KONOSHIMA,
Katsumi KONDO[c] and Fumimichi SANO

Institute of Advanced Energy, Kyoto University, Gokasho, Uji 611-0011, Japan

[b]National Institute for Fusion Science, 322-6 Oroshi-cho, Toki 509-5292, Japan

[c]Graduate School of Energy Science, Kyoto University, Gokasho, Uji, 611-0011, Japan

[d]Laboratorio Nacional de Fusión, EURATOM-CIEMAT, Madrid 28040, Spain

Heliotron J is a flexible concept exploration facility for the helical-axis heliotron concept, where the bumpiness (ε_b) is introduced as the third measure to control the neoclassical transport in addition to the helicity and toroidicity. The effects of ε_b-control on the plasma performance are investigated in Heliotron J from the viewpoints of the fast ion confinement, global energy confinement and Electron-Cyclotron Current Drive (ECCD). The velocity distribution of fast ions generated by Ion-Cyclotron Range of Frequency (ICRF) heating is measured. In a high-ε_b configuration, higher energy particles are observed for all pitch angles compared to that in a lower-ε_b configuration. This observation indicates that the high-ε_b configuration is preferable for the formation and confinement of the fast ions. The bumpiness effect on the global energy confinement for NBI-only plasmas has been investigated. A favorable energy confinement was obtained in the high-ε_b configurations, which could be attributed to the improvements in the energetic ion confinement in the high-ε_b configuration. A wide configuration scan shows that the EC driven current strongly depends on the magnetic ripple structure at the EC power deposited position, indicating that the EC driven current is closely related to the electron trapping.

1. Introduction

In stellarator/heliotron devices, how to suppress the loss of particles trapped in helical ripples is one of the key issues for fusion plasma confinement. To reduce the ripple-loss, the advanced stellarator concepts try to improve the particle orbit through recovering the symmetry of the confinement field (quasi-symmetry concept) or tailoring the Fourier harmonics of the confinement field (quasi-omnigeneous concept). The helical-axis heliotron concept [1] is a new heliotron concept, where the idea based on the omnigeneous concept is introduced keeping a continually wound helical coil(s) for realization of the confinement field.

The Heliotron J device with an $L/M = 1/4$ helical coil [2, 3] is a flexible concept exploration facility for the helical-axis heliotron concept, where the bumpiness ε_b ($= B_{04}/B_{00}$) is introduced as the third measure to control the neoclassical transport in addition to the other major field harmonics in the Boozer coordinates, helicity ($\varepsilon_h = B_{14}/B_{00}$) and toroidicity ($\varepsilon_t = B_{10}/B_{00}$). Here, B_{mn} is the Fourier component with the poloidal and toroidal mode numbers of m and n, respectively. From a viewpoint of the drift optimization, the bumpiness control has an important role in this concept [4].

The configuration control studies are essential parts of the Heliotron J experiment since one of the major objectives of the Heliotron J project is to confirm the effects of the new ideas adopted in this concept and to extend the understanding of the related roles of configuration parameters such as the rotational transform (ι), the field harmonics, magnetic well, magnetic shear, etc. in transport reduction, MHD activity control and/or non-inductive toroidal current control in the omnigeneous optimization scenario.

The ECH-only or ECH+NBI combination plasma experiments in Heliotron J have revealed the existence of windows in the vacuum edge rotational transform $\iota(a)_{vac}$ for the high quality H-mode [5]. Here, $\iota(a)_{vac}$ is used just as a label of the field configuration since $\iota(r)$ can be modified by the existence of plasma. For example, even for non-Ohmic heating plasmas in a stellarator/heliotron device, non-inductive current can be driven by the

pressure gradient (bootstrap current), electron cyclotron current drive (ECCD) and neutral beam current drive (NBCD), etc. The modification of $\iota(r)$ due to such non-inductive plasma currents not only create new rational surfaces in the core region but also modify the edge field structure. The modification of the edge field topology and divertor plasma distribution caused by such non-inductive current has been observed in Heliotron J [6]. Moreover recent NBI-only plasma experiments suggest the causal relation between the onset of the transition to an improved confinement mode and $\iota(r)$ modification due to the plasma current [7, 8]. Since it has been observed that the bootstrap current and ECCD current are affected by the bumpiness tailoring [9, 10], more detailed study of bumpiness effects on the non-inductive current formation is required from a viewpoint of configuration control. On the other hand, the previous ε_b-control experiments indicated that the fast ion confinement produced by NBI or ICRF heating is better in higher ε_b configuration [11, 12], which is qualitatively consistent with the expectation from the drift optimization viewpoint. As for the ε_b-effects on the bulk plasma performance, however, we have observed different dependences between NBI- and ECH-only plasmas. It is necessary to make it clear the role of the bumpiness control in the anomalous and neoclassical transport, and, therefore, in the confinement improvement.

This paper reports recent studies of the configuration effects, especially focusing on the bumpiness control effects, on the plasma performance in Heliotron J. After the short introduction and explanation of the experimental setup, the bumpiness effects on the fast ions generated by ICRF and on the global energy confinement in NBI-only plasma are discussed in Section 3.1 and 3.2, respectively. The bumpiness effect on ECCD is discussed in Section 3.3 from the view point of the field ripple structure at the power deposition area. The summary is given in Section 4.

2. Experimental setup

The details of the Heliotron J device ($\langle R_0 \rangle = 1.2$ m, $B_0 \leq 1.5$ T) is described in [2, 3]. The top view of the plasma ring shows a square shape with four "straight" and "corner" sections as shown in Fig. 1, where the toroidal shape of the $\rho = 0.9$ magnetic-surface for the standard configuration of Heliotron J is illustrated. The color index indicates the strength of the confinement field |B|. At the corner section, where |B| decreases along the major radius like that in tokamaks, while at the straight section, it is designed to make a weak saddle type field gradient.

The field configuration is controlled by using the five sets of the external coils, the helical coil (HV), two individual sets of the toroidal coils (TA and TB) and two sets of the vertical field coils (AV and IV). The bumpiness is mainly controlled by changing the current ratio of TA and TB coils, I_{TA} and I_{TB}, respectively. Trimming of the
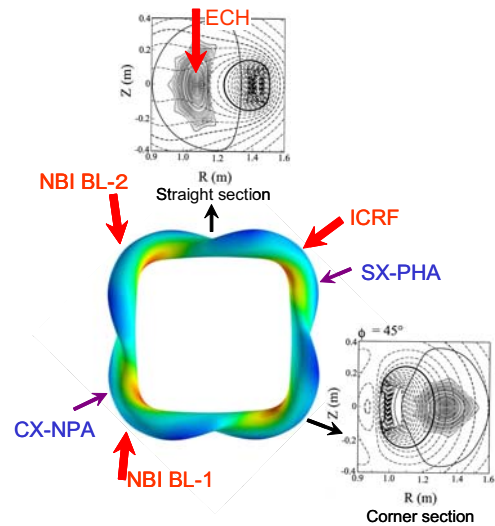
Fig.1 Top view of the magnetic-surface shape (at $\rho = 0.9$) for the standard configuration. The nested magnetic surfaces and the mod-B surfaces at two poloidal sections (straight and corner sections) are also illustrated.

vertical field can make it possible to control ε_b within tolerable deformations of ε_h and ε_t, $\iota(a)_{vac}$, the plasma volume and the averaged major radius. On the other hand, the rotational transform can be controlled by mainly changing the current ratio of the helical to the toroidal coils. Here, it is possible to minimize the change of ε_b by keeping the current ratio of $I_{TA}:I_{TB}$ to be constant.

The initial plasma is produced by using the second harmonic X-mode ECH (70 GHz, < 0.45 MW) launched from a top port located at one of the straight sections. The hydrogen neutral beam (< 30 keV, < 0.7 MW/beam-line) is injected using two tangential beam-lines facing each other (BL-1 and BL-2). Selecting one of the two beam-lines or changing the direction of the confinement field, Co- or CTR-injection is performed. ICRF heating is performed by using two sets of loop antenna installed on the low-field side at a corner section of the torus ($f_{ICRF} \sim 19$-23 MHz, P_{inj} < 0.4 MW/antenna). The locations of heating equipments are also shown in Fig. 1.

3. Bumpiness control experiments

For the bumpiness control experiments, we have selected three configurations with ε_b = 0.15 (high-ε_b), 0.06 (medium-ε_b) and 0.01 (low-ε_b) at $\rho = 2/3$ [13]. Here, the magnetic axis position at the ECH launching section, the plasma volume (≈ 0.7 m^3), the edge rotational transform ($\iota(a)_{vac} \cong 0.56$) are kept almost constant. The standard configuration of Heliotron J corresponds to the medium-ε_b case. Figure 2 shows the variation of the magnetic field strength along the magnetic axis for several ε_b configurations as a function of the toroidal angle, where the field strength at the straight section ($\phi = 0°$) is set constant to keep the ECH resonance condition. The DCOM [14] calculation indicates that the numerical sequence of
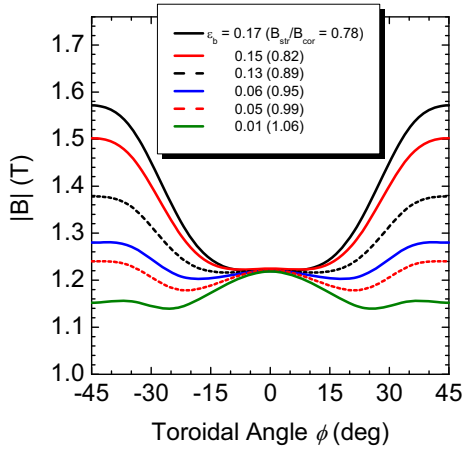
Fig.2 Variation of the magnetic field strength along the magnetic axis for several ε_b configurations.

The toroidal angle of 0° and ±45° correspond to the straight and the corner sections, respectively.

the "effective helical ripple", ε_{eff}, [15] for the three configurations is not the same as that of ε_b, i.e., ε_{eff}'s at $\rho = 2/3$ for the low-, medium- and high-ε_b configurations are 0.26, 0.13 and 0.22, respectively.

3.1. Velocity distribution of fast ions generated by ICRF heating

The fast ion formation/confinement by ICRF heating has been studied in the minority heating scenario (The majority species is deuterium and the minority one is hydrogen.). In the previous experiments, the good confinement of fast ions and the high efficiency of ICRF heating in the high-ε_b case were observed [11-12, 16]. Recently, more detailed comparison between these configurations on the pitch angle dependence of energy spectra for H^+/D^+ has been performed with a charge-exchanged neutral particle energy analyzer (CX-NPA) installed about 180° toroidally apart from the antenna section (see Fig. 1.). The ICRF pulse of 23.2 MHz ($P_{ICRF} \sim 0.27$ MW) is injected into low density ECH target plasmas. The line averaged density, the electron and ion temperatures of the target plasmas are $\bar{n}_e \approx 0.4 \times 10^{19}$ m^{-3}, $T_e(0) \sim 0.8$ keV and $T_i(0) \sim 0.2$ keV, respectively.

Figure 3 shows the energy spectra of the minority ions for various pitch angles in (a) high- and (b) medium-ε_b cases, respectively. Here, the pitch angle of the observed ions was adjusted by toroidally tilting the sight line of the CX-NPA. In the high-ε_b case, the higher energy particles are detected for the whole range of observed pitch angle compared to those in the medium-ε_b case. The hydrogen flux up to 34 keV is observed at the pitch angle of 120°. Such high energy particles, however, cannot be identified in the medium-ε_b case.

In both the configurations, the higher energy flux is detected at the pitch angle of ~ 120° although the ions should be accelerated in the perpendicular direction (~ 90°) by ICRF heating. A Monte Carlo simulation, which takes
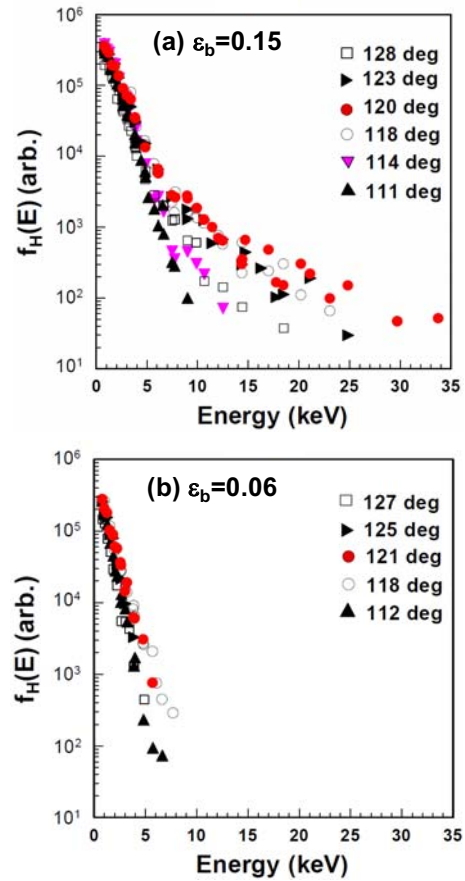
Fig.3 Energy spectra of minority ions (H) for various pitch angles (a) in the high bumpy configuration and (b) in the medium bumpy configurations.

into account the effects of the orbit motion in the real space, pitch-angle and energy scatterings in the velocity space and ICRF heating of test particles (the minority protons), shows that the high energy ions are preferentially observed near 60° and 120° in pitch angle for both the cases and that the amount of higher energy flux seems to be larger in the high-ε_b configuration than that in the medium-ε_b case [17]. Although the experimental data at the pitch-angle of ~ 60° are not available so far, this simulation result is qualitatively consistent with the experimental results. The fast-ion decrease towards 90° observed in the experiment is consistent with the simulation result. This would be mainly due to the existence of the loss region around the perpendicular direction in a low-β condition of these configurations [16].

These observations indicate that the high-ε_b configuration is preferable from the viewpoint of the formation and confinement of fast ions.

3.2. Bumpiness effect on the global energy confinement in NBI-only plasma

As for the ε_b-effects on the bulk plasma performance, we have observed different ε_b-dependences on the global energy confinement between NBI- and ECH-only plasmas. For NBI-only plasma, relatively higher stored energy is obtained in higher ε_b case compared to that in lower ε_b case

[18]. For ECH-only plasmas, however, the best performance is observed not in the high-ε_b but in the medium-ε_b configuration [13, 19]. Figure 4 shows the plasma stored energy measured with a diamagnetic coil
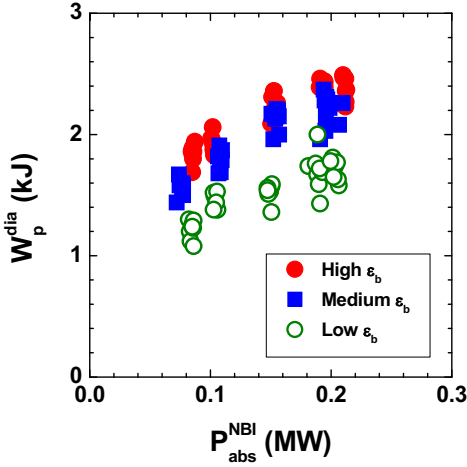
Fig.4 Stored energy obtained in high-, medium- and low-ε_b configurations as a function of absorbed beam power for NBI-only plasmas.

(a)

(b)
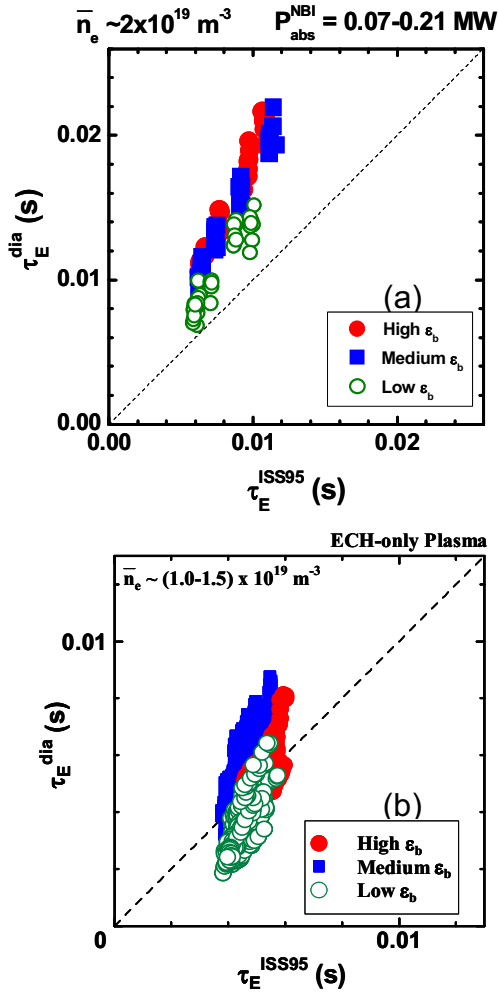
Fig.5 Comparison between τ_E^{dia} and τ_E^{ISS95} for (a) NBI-only plasmas and (b) ECH-only plasma.

system, W_p^{dia}, as a function of the absorbed NB power (P_{abs}^{NBI}) for the high-, medium- and low-ε_b configurations [20]. Here, the H^0-beam is injected tangentially into deuterium plasma after the plasma initiation by a short pulse of ECH. To compare the data for non-transition plasmas even in higher input power condition, NB is injected to the CTR-direction, where no "L-H" transition phenomena [5] have been observed so far [7, 8]. These data were obtained at $\bar{n}_e \approx 2 \times 10^{19}$ m^{-3}. The beam absorption profile is evaluated by FIT [21] and the orbit-loss fractions in the high-, medium- and low-ε_b cases are 25%, 26% and 29%, respectively. The NBI plasma discussed here is in the plateau regime of the collisionality. As shown in the figure, W_p^{dia} in the high- and medium-ε_b configurations is clearly high compared to that in the low-ε_b case. The difference between the high- and medium-ε_b is not so clear but W_p^{dia} in the high-ε_b configuration seems higher than that in the medium-ε_b one. To take into account the differences in $\langle R \rangle$, $\langle a_p \rangle$ and $|B|$ for these configurations, the comparison of the experimentally evaluated global energy confinement time (τ_E^{dia}) with the International Stellarator Scaling (τ_E^{ISS95}) is plotted in Fig. 5(a). Also from this comparison, it is found that the data for the high- and medium-ε_b configurations are better than those for the low-ε_b case.

Since the data plotted in Fig. 5(a) are obtained at the same $\bar{n}_e$ condition, the difference in W_p^{dia} (or τ_E^{dia}) should be attributed to the difference in temperature. Actually, the bulk ion (D^+) temperature, which is evaluated with the CX-NPA, increases as increase of ε_b; the ion temperature in the high-, medium- and low-ε_b cases were 0.23, 0.20 and 0.18 keV, respectively, at $P_{abs}^{NBI} \approx 200$ kW. Moreover, the signal intensity of the electron cyclotron emission (I_{ECE}) from the core region also indicates the higher electron temperature in higher ε_b case as shown in Fig. 6. As increasing P_{abs}, I_{ECE}'s in high- and medium-ε_b cases are increased, while the dependence of I_{ECE} on P_{abs}^{NBI}
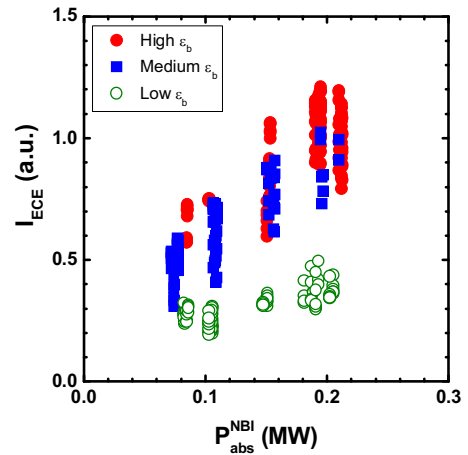
Fig.6 ECE intensity as a function of P_{abs}^{NBI} in high-, medium- and low-ε_b configurations.

is weaker in the low-ε_b configuration.

The similar comparison of τ_E^{dia} for ECH-only plasmas is plotted as Fig. 5(b) for reference. For ECH-only plasmas, only the data of $\bar{n}_e \approx (1.0-1.5)\times10^{19}$ m^{-3} are plotted from the database to exclude the H-mode data. The lower density ($\bar{n}_e < 1.0\times10^{19}$ m^{-3}) data are also excluded. The data for ECH-only plasmas show that the best performance is observed in the medium-ε_b case, which has the lowest ε_{eff} in the examined three configurations, and the difference between the high- and low-ε_b cases is not so clear in this density range.

To understand the observed difference in the ε_b-dependence of τ_E^{dia} (or W_p^{dia}) between NBI- and ECH-only plasmas, we should consider two possibilities besides the density dependence; one is the difference in the ε_b-dependence of the transport and the other is that in the "heating efficiency." Since a different heating method might cause a different radial electric field structure in the plasma, the difference of the transport should be discussed taking into account the effect of the radial electric field. As for the latter possibility, we have found in the previous experiments that the characteristic decay time of the high energy CX flux after turning-off of NBI became longer as increasing bumpiness [11]. Since the heating source is only the fast ions in NBI-only plasmas, the improved confinement of the energetic ions would contribute to increase the plasma temperature. Therefore, it is considered that the improved confinement of the energetic ions would increase the plasma temperature and raise the plasma performance in the high-ε_b configuration. In the low-ε_b configuration, on the other hand, the less heating due to the poor confinement of the energetic ions might enhance the degradation in the plasma performance between these configurations. More detailed studies are under progress.

3.3. Effect of magnetic field ripple on ECCD

The ripple structure of the magnetic field near the power absorption position should be one of the key factor
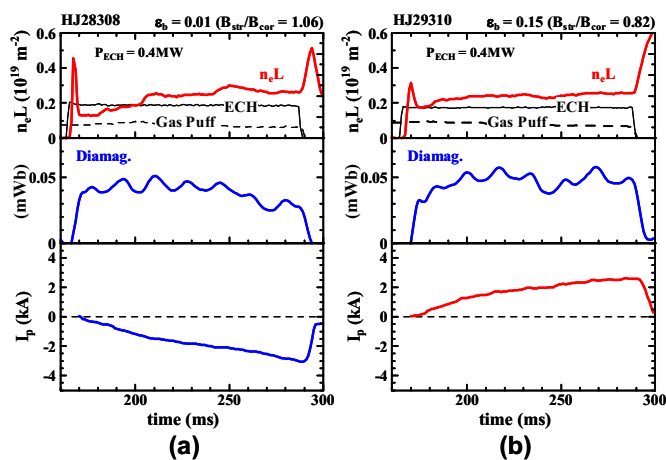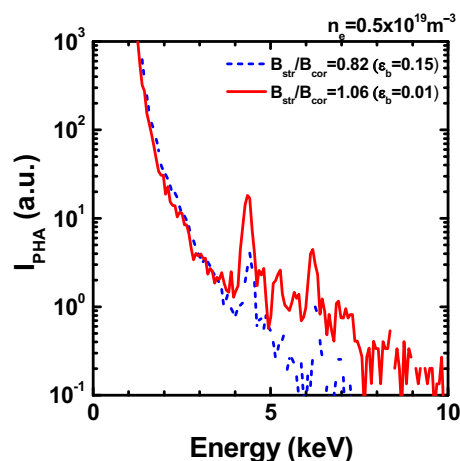
Fig.8 SX spectra for ripple-top (B_{str}/B_{cor} = 0.82) and ripple-bottom (B_{str}/B_{cor} = 1.06) heating cases.

in ECCD when the ECCD results from the balance between the Fisch-Boozer [22] and Ohkawa effects [23].

Recently, a wide scan experiment of the ripple ratio of the magnetic field has been performed to study its effect on ECCD [24]. At the present launching condition of microwaves in Heliotron J, the launched beam crosses the resonance layer with a finite parallel refractive index $N_{\|}$ of ≈ 0.44. In this experiment, the injected power P_{ECH} is up to 0.44 MW, and the maximum pulse length is 0.16 s. The electron and ion temperatures are in the ranges 0.3-1.0 keV and 0.15-0.2 keV, respectively. The field strength is adjusted to satisfy $\omega_0/\omega = 0.49$ since the TRECE code [25] predicts that the EC power is deposited on the axis at this case due to the Doppler shift of the resonance condition. Here ω_0 is the electron cyclotron frequency on the axis at the launching section and ω is the injected wave frequency. Actually the maximum electron temperature is observed at this condition.

Figure 7 shows the time traces of electron density, diamagnetic signal and non-inductive toroidal plasma current for (a) the low- and (b) high-ε_b configurations. The direction of the observed plasma current in the high-ε_b case is opposite to that in the low-ε_b case. In this plasma density ($\bar{n}_e \approx 0.5\times10^{19}$ m^{-3}), the contribution of bootstrap current is considered to be less than +0.5 kA [10].

A wide scan experiment of the ripple ratio indicates that the observed toroidal current I_p is a function of the magnetic field ripple B_{str}/B_{cor} under the fixed condition of P_{ECH}. Here B_{str}/B_{cor} denotes the ratio of the field strength on the magnetic axis at the straight and corner sections and is closely related to ε_b. In the condition of B_{str}/B_{cor} = 1.06 (ε_b = 0.01), where the EC power is deposited at the ripple top position as shown in Fig. 2, the EC driven current flows in the clockwise direction (negative in Fig. 7). This direction is consistent with the direction of EC driven current due to the Fisch-Boozer effect. As decrease of B_{str}/B_{cor} (i.e. as increase of ε_b), the EC power deposition relatively shifts to the ripple bottom. Following to this shift, the observed current gradually

Fig.7 Time traces of electron density, diamagnetic signal and non-inductive toroidal plasma current for (a) the low- and (b) high-ε_b configurations in the ECCD experiment. ($\omega_0/\omega \approx 0.49$)

decreases, and finally changes its direction to the counter-clockwise direction (the direction expected from the Ohkawa-effect) as shown in Fig. 7(b).

The change of B_{str}/B_{cor} should have an effect on the trapping of electrons accelerated by ECH. Figure 8 shows soft X-ray spectra measured with a PHA system at the adjacent section of the torus (see Fig. 1) for B_{str}/B_{cor} = 0.82 and 1.06 cases. Although careful discussions are necessary on the effects of line emissions in these energy spectra, higher energy tail seems to exist in the B_{str}/B_{cor} = 1.06 case compared to the B_{str}/B_{cor} = 0.82 case. This suggests that, in the ripple bottom heating case, the higher energy electrons accelerated by ECH are trapped due to their high pitch angle but they can move around the torus when the EC power is deposited at the ripple top (the B_{str}/B_{cor} = 1.06 case). This experiment suggests that the EC driven current is closely related to the trapping of the accelerated electrons. The efficiency of ECCD is discussed in [26].

4. Summary

An overview of recent investigations into the effects of the configuration control on the plasma performance in Heliotron J is described.

The velocity distribution of the minority ions in the ICRF minority heating is investigated for low-density ECH target plasmas with special emphasis on the effect of the bumpiness. The experimental observations indicate the preferable characteristic of the high-ε_b configuration for the formation and confinement of the fast ions.

The effect of the bumpiness on the global energy confinement for NBI-only plasmas has been investigated. A favorable energy confinement was obtained not only in the medium-ε_b configuration, which shows better global energy confinement for ECH-only plasma than the high- or low-ε_b configuration, but also in the high-ε_b configurations. It is considered that the improved confinement of the energetic ions increases the plasma temperature and raises the plasma performance in the high-ε_b configuration.

A wide configuration scan experiment shows that the EC driven current strongly depends on the magnetic ripple structure at the EC power deposited position, indicating that the EC driven current is closely related to the trapping of the accelerated electrons.

Acknowledgement

[1]   M. Wakatani, et al., Nucl. Fusion **40**, 569 (2000).
[2]   F. Sano, et al., J. Plasma Fusion Res. SERIES 3, 26 (2000).
[3]   T. Obiki, et al., Nucl. Fusion **41**, 833 (2001).
[4]   M. Yokoyama, et al., Nucl. Fusion **40**, 261 (2000).
[5]   F. Sano, et al., Nucl. Fusion **45**, 1557 (2005).
[6]   T. Mizuuchi, et al., Nucl. Fusion **47**, 395 (2007).
[7]   S. Kobayashi, et al., in 11th IAEA TM on H-mode Phys. Trans. Barriers (Tsukuba, 2007).
[8]   T. Mizuuchi, et al., Joint Conf. "17th Int. Toki Conf. on Phys. Flows & Turbulence in Plasmas" and "16th Int. Stellarator/Heliotron Workshop" (Toki, 2007) O-02.
[9]   G. Motojima, et al., Fusion Sci. Tech., **51**, 122 (2007).
[10]   G. Motojima, et al., Nucl. Fusion **47**, 1045 (2007).
[11]   S. Kobayashi, et al., IAEA-CN-116/EX/P4-41 (2004)..
[12]   H. Okada, et al., Fusion Sci. Tech.. **50**, 287 (2006).
[13]   T. Mizuuchi, et al., Fusion Sci. Tech. **50**, 352 (2006).
[14]   A. Wakasa, et al., J. Plasma Fusion Res. **4**, 408 (2001).
[15]   V. V. Nemov, et al., Phys. Plasmas **6**, 4622 (1999).
[16]   H. Okada, et al., Nucl. Fusion **47**, 1346 (2007).
[17]   H. Okada, et al., in 22nd IAEA Fusion Energy Conference, "Velocity Distribution of Fast Ions Generated by ICRF Heating in Heliotron J", (Geneva, 2008) EX/P6-28. to be submitted to Nucl. Fusion.
[18]   S. Kobayashi, et al., in 2nd Joint Meeting of US-Japan Workshop and Kyoto Univ. the 21st COE Sympo. "New approach in Plasma Confinement Exp. in Helical Systems", (Auburn, USA, 2006).
[19]   F. Sano, et al., IAEA-CN-149/EX/5-5Ra (2006).
[20]   S. Kobayashi, et al., in 2nd IAEA Fusion Energy Conference, "Effect of Bumpy Magnetic Field on Energy Confinement in NBI Plasmas of Heliotron J", (Geneva, 2008) EX/P5-13. to be submitted to Nucl. Fusion.
[21]   S. Murakami, et al., Trans. Fusion Tech. **27**, 259 (1995).
[22]   N. J. Fisch, A. H. Boozer, Phys. Rev. Lett. **45**, 720 (1980).
[23]   T. Ohkawa, General Atomics Report GA-A13837 (1976).
[24]   K. Nagasaki, et al., in 2nd IAEA Fusion Energy Conference, "Effect of Magnetic Field Ripple on ECCD in Heliotron J", (Geneva, 2008) EX/P6-15. to be submitted to Nucl. Fusion.
[25]   V. Tribaldos, et al., J. Plasma Fusion Res. **78**, 996 (2002).
[26]   G. Motojima, et al., in this conference, BET.P1-205.